analytical chemistry

pubs.acs.org/ac Article

Surface-Induced Dissociation of Protein Complexes Selected by Trapped Ion Mobility Spectrometry

Erin M. Panczyk, Dalton T. Snyder, Mark E. Ridgeway, Árpád Somogyi, Melvin A. Park, and Vicki H. Wysocki*

Cite This: *Anal. Chem.* 2021, 93, 5513−5520 Read Online

ACCESS | Metrics & More | Article Recommendations | Supporting Information

ABSTRACT: Native mass spectrometry (nMS), particularly in conjunction with gas-phase ion mobility spectrometry measurements, has proven useful as a structural biology tool for evaluating the stoichiometry, conformation, and topology of protein complexes. Here, we demonstrate the combination of trapped ion mobility spectrometry (TIMS) and surface-induced dissociation (SID) on a Bruker SolariX XR 15 T FT-ICR mass spectrometer for the structural analysis of protein complexes. We successfully performed SID on mobility-selected protein complexes, including the streptavidin tetramer and cholera toxin B with bound ligands. Additionally, TIMS−SID was employed on a mixture of the peptides desArg1 and desArg9 bradykinin to mobility-separate and identify the individual peptides. Importantly, results show that native-like conformations can be maintained throughout the TIMS analysis. The TIMS−SID spectra are analogous to SID spectra acquired using quadrupole mass selection, indicating little measurable, if any, structural rearrangement during mobility selection. Mobility parking was used on the ion or mobility of interest and 50−200 SID mass spectra were averaged. High-quality TIMS−SID spectra were acquired over a period of 2−10 min, comparable to or slightly longer than SID coupled with ion mobility on various instrument platforms in our laboratory. The ultrahigh resolving power of the 15 T FT-ICR allowed for the identification and relative quantification of overlapping SID fragments with the same nominal m/z based on isotope patterns, and it shows promise as a platform to probe small mass differences, such as protein/ligand binding or post-translational modifications. These results represent the potential of TIMS−SID−MS for the analysis of both protein complexes and peptides.

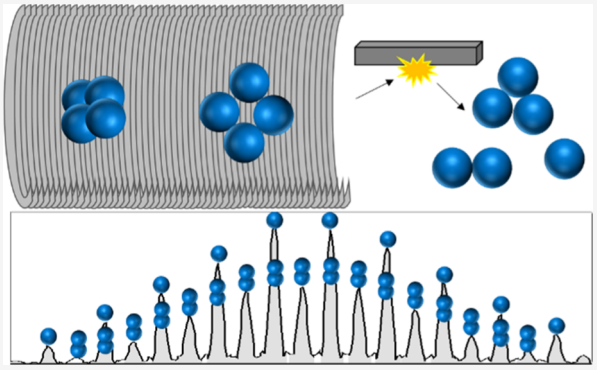

INTRODUCTION

Proteins often carry out their functions as complexes of multiple proteins. The understanding of their assembly is integral to determine how the architecture affects function and possibly malfunction. Traditional biophysical methods, such as NMR, cryo-electron microscopy, or X-ray crystallography, are useful tools for probing the structures and dynamics of biological molecules.[1−4] Native mass spectrometry (nMS), particularly in conjunction with gas-phase ion mobility measurements, offers complementary information for evaluating the stoichiometry, conformation, and topology of protein complexes. The information provided and its sensitivity and ease of use have made nMS a rapidly growing technique for analyzing proteins and protein complexes prepared in solutions that mimic the cellular environment, thus maintaining their native-like structure.[1,2] These biological systems are efficiently ionized, under low voltage and low activation instrument conditions, and transferred to the gas phase using nano-electrospray ionization (nESI) in kinetically trapped, native-like structures, in which structural disruption is limited and noncovalent interfaces are preserved.[3] Importantly, nMS is capable of probing multiple conformations and proteoforms of protein complexes with low sample amounts, less-extensive sample preparation, and relatively uncomplicated data processing.[5−7] The combination of ion mobility spectrometry (IMS) and surface-induced dissociation (SID) in a single nMS experiment provides a wealth of structural information for protein complexes, including conformational landscape information and subunit stoichiometry, connectivity, and topology.[8−11]

IMS provides an extra dimension of structural characterization when coupled with MS by separating ions not only by mass but also by their rotationally averaged collision cross-sections.[11−20] There are several different ion mobility methods and instrument types available, and these have been compared

Received: December 22, 2020
Accepted: March 5, 2021
Published: March 22, 2021

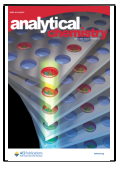

https://doi.org/10.1021/acs.analchem.0c05373
Anal. Chem. 2021, 93, 5513−5520

in depth previously.[20] Both drift tube IMS (DTIMS) and traveling wave IMS (TWIMS) have been utilized regularly by the nMS community for the analysis of protein complexes. In linear cell DTIMS, a potential is applied along the ion mobility cell, while ions are accelerated into a quasi-stationary bath gas, providing a drag force that opposes the ion motion along the potential gradient.[21−23] As a result, larger or more expanded ions undergo a greater number of collisions, therefore taking longer to traverse the IMS cell compared to more rigid or compact conformations. For ions of the same m/z, more compact ions, described as having higher mobility, will exit from the IMS cell sooner compared to expanded ions.

Trapped IMS (TIMS), initially optimized and implemented for small molecules, has been gaining traction for the analysis of native proteins and protein complexes.[24,25] TIMS differs from the previously mentioned techniques in that an electric field that opposes the ion motion is used to hold ions stationary against a bath gas which pushes ions along the TIMS analyzer (an ion funnel). Ions of different mobilities are trapped at different points (potentials) along the ion optical axis using the electric field gradient and are then eluted from the device over time, based on their mobility, as the TIMS potential gradient is reduced.[26−29] Because the bath gas flows in the same direction as the ions, larger or more expanded ions are trapped farther along the TIMS analyzer and exit sooner than smaller or compact ions. Because ions are trapped and separated in the TIMS funnel, resolving power and time of analysis can be user-defined and optimized for a given application. For example, if high resolving power is necessary to separate two ions of similar mobilities, the step size of the voltage profile (or slope) is decreased and overall time of analysis increased. For species requiring less resolving power, the voltage profile is stepped at larger increments and overall analysis time is much shorter, allowing for rapid analysis. Because the resolving power of TIMS is not limited to IMS analyzer length, as are the traditional drift tube or traveling wave ion mobility, higher mobility resolution has been achieved with TIMS. Park and co-workers observed a resolving power of up to ∼300 for separation of ubiquitin conformations, allowing for the identification of several additional conformations previously undetected using DTIMS (R = 20−50).[19,30−33] The use of quadrupolar RF confinement in the TIMS funnel also decreases the radial spread and loss of ions compared to a traditional dc-only drift cell analyzer, therefore increasing the total ion signal and allowing for ion activation of mobility-separated ions.[34] This is important in the results described here because having a confined and well defined ion beam after mobility analysis facilitates surface collision experiments.

SID is a gas-phase activation technique that can probe protein complex stoichiometry, connectivity, subunit interactions, and structural rearrangements.[35−40] To perform SID, ions are intentionally accelerated toward a rigid surface in the mass spectrometer. The result of the collision is a rapid increase in internal energy that often results in compact fragments indicative of the native topology of the complex, that is, non-covalent bonds are cleaved to separate subcomplexes at the weaker one of multiple interfaces. Most commercially available tandem mass spectrometers are equipped with gas-phase collision-induced dissociation (CID) capabilities, in which ions undergo numerous, low-energy collisions with neutral gas molecules.[40] CID can restructure protein complexes in a variety of ways that can include collapse or expansion/unfolding, often yielding a highly charged monomer and the corresponding $(n - 1)$mer, therefore limiting the amount of structural information gained from these experiments.[19] SID can access higher energy pathways with minimal restructuring, a pathway often unattainable by multi-step activation in CID, with SID often yielding lower charge, compact subunits with symmetric charge partitioning. The implementation of SID capabilities on a Bruker SolariX XR 15 T FT-ICR,[42−45] capable of high mass resolving power, has proven extremely beneficial for identifying overlapping oligomers produced from SID (i.e., dimer 4+ and monomer 2+) and probing small mass/charge differences, such as ligand binding or post-translational modifications.[36]

TIMS combined with SID can be used to probe conformational dynamics, such as whether specific conformations can be identified as native-like, collapsed, or expanded (including unfolding). With the typical symmetric charge partitioning of SID (and occasional/atypical symmetric charge partitioning of CID),[46] product ions often overlap in the m/z space, requiring another stage of separation for identification. The ultrahigh resolving power of the FT-ICR, however, allows for the identification of overlapping oligomers based on their isotope patterns. Here, we present the implementation and evaluation of TIMS combined with SID for the protein complexes streptavidin and cholera toxin B (CTB) with the GM1s ligand (sugar head group of GM1) and a peptide mixture of desArg1 and desArg9 bradykinin on a 15 T FT-ICR mass spectrometer.

METHODS AND MATERIALS

Sample Preparation. Ammonium acetate, ethylenediamine diacetate (EDDA), CTB, the sodium salt of the pentasaccharide Galβ1-3GalNAcβ1-4(Neu5Ac-α2-3)-Galβ1-4Glc (GM1s), and desArg1 (PPGFSPFR) and desArg9 (RPPGFSPF) bradykinin were purchased from Sigma-Aldrich (St. Louis, MO). Streptavidin from *Streptomyces avidinii* was purchased from Thermo Scientific Pierce Biotechnology (Rockford, IL) and has the known issue that each protein monomer has zero or one methionine at the N-terminus. Protein complexes were buffer-exchanged twice into 200 mM ammonium acetate (pH near neutral) with size exclusion chromatography spin columns (Micro Bio-Spin 6, Bio-Rad, Hercules, CA). EDDA was used as a charge-reducing agent and added to protein solutions at a final concentration of 40 mM EDDA and 160 mM ammonium acetate. Final protein concentrations ranged from 5 to 10 μM. For the desArg1 and desArg9 bradykinin mixture, the peptides were mixed at equal concentrations in 1:1 water/acetonitrile, at a final concentration of 5 μM each.

Instrumentation. All experiments were performed on a Bruker SolariX XR 15 T FT-ICR mass spectrometer (depicted in Figure 1, Bruker Daltonics, Bremen, Germany). Ions for MS experiments were generated using nESI. Static nESI capillaries were prepared in-house using Sutter Instrument thin-wall borosilicate capillaries with a filament (outside diameter = 1.00 mm and inside diameter = 0.78 mm) and a Sutter Instrument P-97 Flaming/Brown-type micropipette puller (Novato, CA). Capillary voltages of 0.6−1.1 kV were used for nESI via a 0.25 mm-diameter platinum wire (Sigma Aldrich, St. Louis, MO) inserted into the back of the capillary with a temperature of 180 C and 5 L/min drying gas flow rate.

Once in the vacuum system, ions may be analyzed and manipulated in a variety of ways. A prototype TIMS analyzer (Figure 1A) is incorporated in the first pumping region—

https://doi.org/10.1021/acs.analchem.0c05373
Anal. Chem. 2021, 93, 5513−5520

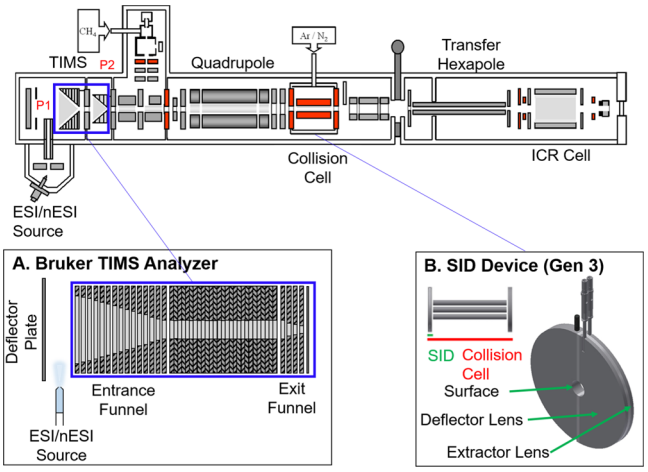

Figure 1. Instrument design and modifications, including a TIMS analyzer[29] (A) and SID device[42] (B). The TIMS analyzer replaced the entrance funnel (original entrance funnel region shown in the blue box was replaced with the TIMS analyzer as shown in the bottom blue box) and the SID device replaced the front endcap of the commercial collision cell. The previously described SID device consists of three lenses: a semicircular surface onto which ions collide and two lenses with a non-conducting space in between: a deflector lens to push ions into the surface and an extractor lens element to extract and guide ions into the collision cell for accumulation prior to being pulsed into the ICR cell for detection.[42]

serving the dual purpose of collecting the ions for transmission to downstream pumping stages and mobility analyzing the ions. The ions may also be mass filtered in an analytical quadrupole before arriving at the SID optic (Figure 1B). The ions may either be SID-activated or allowed to pass unactivated into the collision cell. Typically, ions are collected in the collision cell before being transmitted to the ICR cell for mass analysis.

Surface-Induced Dissociation. The front endcap of the standard Bruker collision cell was replaced with a split lens SID device, termed as "Gen 3" and described in a recent manuscript.[42] Gen 3 consists of three electrodes: a surface, deflector, and extractor lens (Figure 1B).[42] The device can be operated in both SID and transmission modes. The surface consists of a metal electrode (stainless steel, presumably coated with adventitious organics in the vacuum system). No significant neutralization/ion loss for large multiply charged protein complexes was observed using a stainless-steel surface compared to a gold surface coated with fluorocarbon self-assembled monolayers, as previously described by the Wysocki research group.[42,47] In SID mode, positive ions are accelerated toward the surface by applying an attractive voltage (more negative than the exit of the quadrupole mass analyzer) to the surface while applying a more positive voltage to the deflector (Figure S1). SID energy can be increased by applying an even more negative voltage to the surface electrode, thus increasing the ion acceleration into the surface. After surface collision, the activated ions are extracted directly into the collision cell by applying a voltage to the extractor lens that is equivalent to, or slightly more positive, than the surface voltage while simultaneously holding the collision cell rods at a DC bias lower than that of the surface. SID lab frame collision energies (in eV) are defined as the acceleration voltage (difference between the quadrupole exit lens and surface electrode) multiplied by the charge state of the precursor ion. In transmission mode, the three lenses are set to equivalent potentials, and ions simply traverse the front endcap without any surface collision. The transmission mode also allows for CID experiments in the collision cell without removal or modification of the Gen 3 SID device.

Implementation of TIMS with SID. The ion funnel region was replaced with a custom TIMS analyzer (Bruker, Billerica, MA) equipped with an external power supply (Figure 1A).[30,48] In-house software, written in C++ by Danielson Software Consulting (Richland, WA) utilizing National Instruments LabVIEW resources (Austin, TX), was used to control the TIMS analyzer and was synchronized with the FT-ICR MS data acquisition program using a special pulse program. For TIMS analysis of large protein complex ions (greater than 3000 m/z), the standard 900 kHz RF driver in the source (ion funnel) region was replaced with a 450 kHz RF driver capable of providing up to 300 V_{pp}. Care was taken when setting the RF amplitude as high values can unintentionally activate proteins and protein complex ions. Mobility separation was performed using nitrogen as a bath gas at approximately 300 K with P_1 = 3.2 mbar (entrance of TIMS) and P_2 = 1.4 mbar (exit of TIMS) (Figure 1). The TIMS deflector plate (V_{def}) voltage was set to 150 V for TIMS accumulation (open) and 0 V for the trapping and elution steps (closed) to prevent additional ions from entering the TIMS analyzer. The commercial quadrupole on this instrument has a theoretical upper selection limit of 6000 m/z; however, to perform successful Q-SID experiments, we have observed an experimental upper limit of 4000 m/z due to the lack of a well-defined ion beam and signal beyond this limit. The application of TIMS−SID here represents the ability for selection and activation without modification to the commercial quadrupole. The quadrupole was set to the transmission mode for all experiments reported here; however, if a second mode of separation is required (i.e., overlapping mobilities with different m/z), the quadrupole can be set to the selection mode.

Additionally, the experimental setup includes an ion gate downstream of the TIMS funnel, as previously described elsewhere.[20] Briefly, the ion gate is used to select or eliminate ions of different mobilities, allowing for the coupling of TIMS with the slower FT-ICR mass analyzer.[29] The TIMS analyzer was operated using an accumulate/trap/elute (with gating)/quench sequence over 34 ms per mobility scan. Ions selected with the ion gate are accumulated in the Bruker collision cell before being pulsed into the ICR cell, with an average of 25−100 ion mobility scans per mass spectrum. For the filling step of one TIMS scan, ions were accumulated for 15 ms of the total 34 ms TIMS profile. The TIMS funnel was quenched at the conclusion of each scan before beginning the next. An example of the voltages and timings used in the TIMS ion funnel region can be found in the Supporting Information (Figures S2 and S3). For the streptavidin tetramer, the starting and ending voltages of the TIMS ramp were set to −275 and −50 V, respectively. After completion of a mobility of interest, the voltage profile was lowered to the next mobility of interest.[30] A pictorial representation of the accumulate/trap/elute/quench sequence can be found in Figure 2A. When performing TIMS−SID experiments, the trapping voltage was held constant at the elution voltage for the mobility corresponding to the precursor of interest, resulting in isolation of a selected mobility (referred to as "mobility parking", Figure 2B). Approximately, 50−200 mass spectra were averaged to

https://doi.org/10.1021/acs.analchem.0c05373
Anal. Chem. 2021, 93, 5513−5520

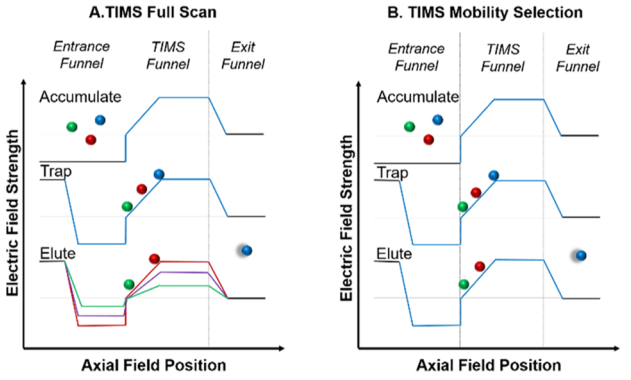

Figure 2. Visual representation of the TIMS voltage profiles used for full scans (A) or mobility selection for SID experiments (B). For the full scan, the voltage is lowered in a stepwise fashion to elute ions of different mobilities as a function of time. For mobility selection, the voltage is set for only the ion of interest to elute. The TIMS funnel is quenched after each mobility scan to remove any remaining ions before beginning the next accumulation step.

yield the multi-dimensional IM−MS spectrum, resulting in an average analysis time ranging from 2−10 min. TIMS−SID required longer averaging time compared to performing SID without mobility selection due to the lower duty cycle of combining TIMS with SID; however, the total experiment time is comparable to SID-IMS experiments performed on our Waters Snyapt Q-SID-TWIMS-TOF mass spectrometers.[41,45] When calibrating TIMS mobility for proteins and protein complexes, two calibration methods were compared to assess the accuracy of Tune Mix for large, globular ions. Elution voltage values of ions were converted to reduced mobilities using both an Agilent Tune Mix calibration curve and a curve constructed using standard proteins and protein complexes (Figure S4). Collision cross-sections were calculated from reduced mobilities (K_o) using the Mason−Schamp equation (eq S1) and compared for both calibration methods (Table S1).

For each sample, an initial full TIMS scan was performed to determine the elution voltage for ions of particular interest, with the Gen 3 SID device held in transmission mode. To perform TIMS−SID experiments, the TIMS voltage ramp was held constant (or "parked") at the elution voltage of interest and the Gen 3 SID device was tuned for SID mode. The collision cell accumulation time was set to a value in the range of 0.6−3.0 s (depending on the number of TIMS accumulations and need for increased ion throughput, similar to Bruker's typical CASI, continuous accumulation of selected ions, mode for CID). Post accumulation, ion packets were pulsed into the ICR cell for detection. The process of pulsing an ion packet into the ICR was performed multiple times and the resulting mass spectra were averaged for a total analysis time of 2−10 min. The time-of-flight setting, which controls the time ions have to travel between the collision cell into the ICR cell, was optimized to ensure a balanced detection of low- and high-m/z ions (typically 2.2−3.0 ms for protein complexes). A low time-of-flight setting results in a bias toward increased detection of low-m/z ions, as high-m/z ions require a longer time of flight. An example of the ICR tune settings used for nMS experiments is provided in Figure S5.

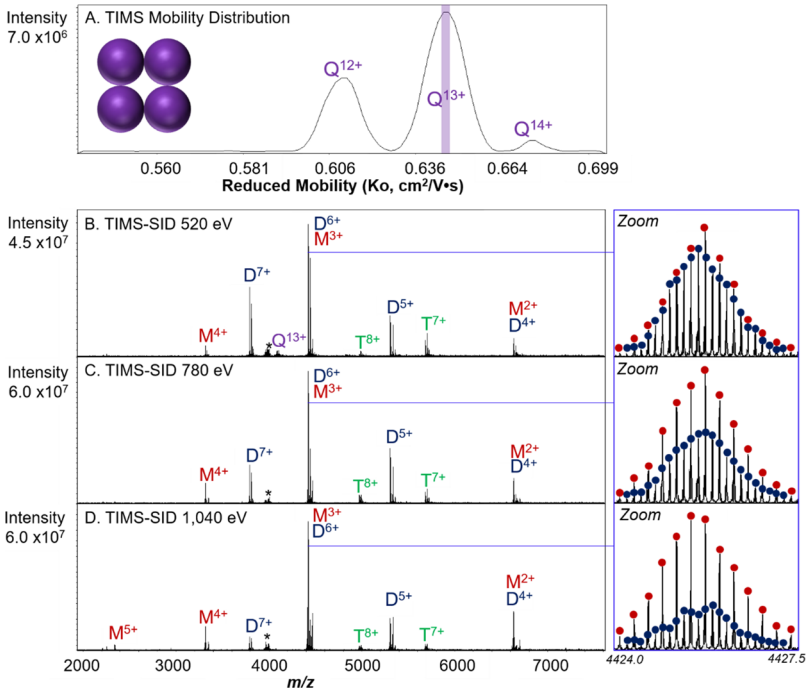

Figure 3. TIMS mobility distribution of the streptavidin tetramer with the mobility selection used for SID experiments highlighted by the purple slice (A). Reduced mobilities were calculated using the protein/protein complex calibration. TIMS−SID of the mobility-selected 13+ streptavidin tetramer at different activation energies. At low SID energy [520 eV (B)], SID yields dimer and monomer products. As SID energy is increased to 780 (C) and 1040 eV (D), trimers are also observed in the mass spectra. Even relatively low mass resolution ($R_{calculated}$ = 138,000) for the 15 T FT-ICR allows for identification of overlapping monomers and dimers based on isotopic distributions, as shown in the zoom-in panels. The ratio of total dimers to [monomer plus trimer] for each energy varies from 85:15 at 540 eV to 16:84 at 1040 eV. The asterisk denotes a noise peak.

https://doi.org/10.1021/acs.analchem.0c05373
Anal. Chem. 2021, 93, 5513−5520

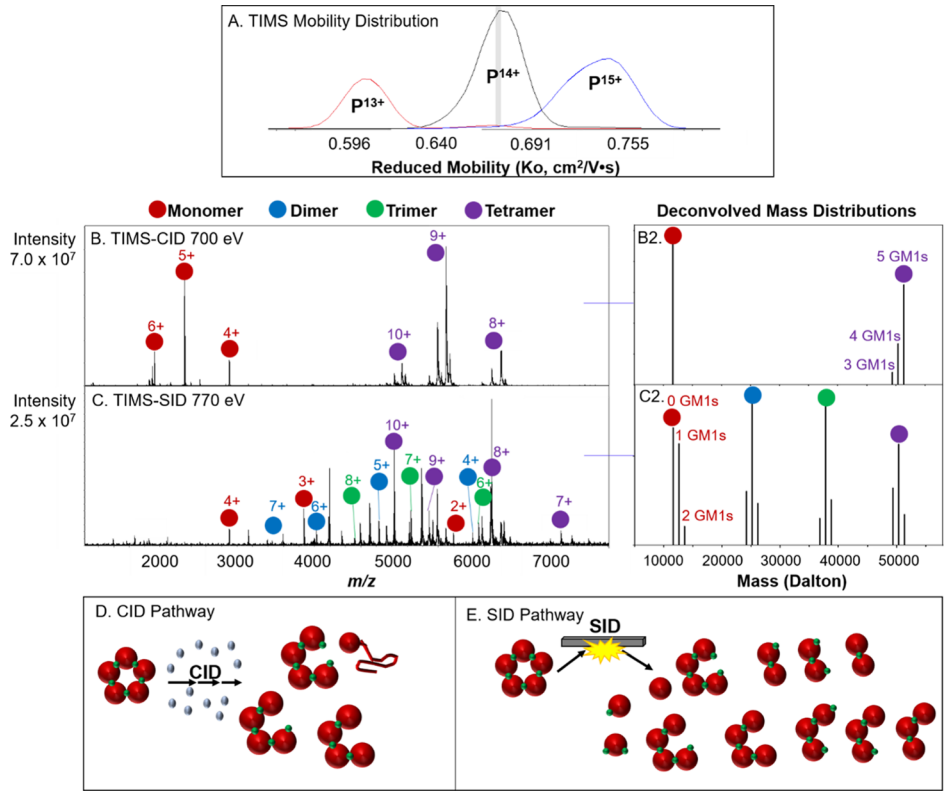

Figure 4. TIMS mobility distribution of the CTB pentamer with GM1s ligands bound with mobility selection for CID and SID experiments highlighted with the gray slice (A). Reduced mobilities were calculated using the protein/protein complex calibration. TIMS−CID and TIMS−SID of mobility-selected 14+ (B,C) with corresponding deconvolution to show variations of GM1s retention on subunits (B2,C2). CID and SID pathways of CTB with GM1s and the observed products (D,E).

RESULTS

Application of TIMS−SID for Biological Samples. *TIMS−SID of the Streptavidin Tetramer.* To validate the performance of TIMS coupled with SID for native MS and optimization of TIMS tuning parameters for high mass trapping and transmission, a series of standard protein complexes were chosen. These systems have been well-characterized with different IMS methods and SID previously.

Streptavidin, a 53 kDa homotetramer, is a dimer of dimers; therefore, SID yields predominately compact dimers at low energies. At higher SID laboratory collision energies, charge-symmetric with respect to mass, and therefore assumed to be, compact monomers and trimers form in competition with the formation of dimers.[49] As provided by Sigma, the streptavidin tetramer contains variable numbers of leading methionines, with zero or one on each monomer; these can be seen in the spectra for both the main series of peaks and for salt adducts. The results of the TIMS−SID−MS analysis of streptavidin are shown in Figure 3. The full mass spectrum for charge-reduced streptavidin can be found in Figure S5. The full TIMS distribution for streptavidin yielded distinct mobility profiles for the 12+, 13+, and 14+ charge states (Figure 3A). In Figure 3B−D, TIMS was used to mobility select the 13+ charge state ($V_{elution}$ = −203 V, K_o—0.64 cm^2 V^{-1} s^{-1}) and then activated at three different SID energies.

TIMS−SID of the mobility-selected Q^{13+} tetramer yields mostly symmetrically charged dimer (on average, half the charge of the tetramer precursor) and symmetrically charged monomer, which can be indicative of compact subunit fragments.[40] As previously mentioned, streptavidin is considered a dimer of dimers; therefore, dissociation based on its native interfaces should occur between the two dimers. As SID energy is increased, however, the complex dissociates into compact, low-charge (5+, 4+, 3+, and 2+) monomers and their complementary trimers (Figure 3). Because of the high resolving power of the 15 T FT-ICR, overlapping oligomers were also identified based on their isotopic distributions. For example, TIMS−SID of streptavidin shown in Figure 3B resulted in the overlapping 3+ monomer and 6+ dimer. The differing amounts of the monomer and dimer can be observed by zooming into the spectra at this region. An increase in SID energy resulted in the production of more monomer products, presumably from dimers that were observed to decrease at higher energies (trimers were of very low abundance at these energies). A comparison between TIMS−SID and TIMS−CID can be found in Figure S7. Here, we obtained high signal-to-noise ratios ($S/N_{m/z\ 4424}$ = 120.3 for streptavidin) for protein complexes, evidenced by the accurate isotopic distributions of species of low abundance.

TIMS−CID and TIMS−SID of the CTB Pentamer (with the GM1s Ligand). TIMS ion mobility instruments operate by holding ions stationary in an electric field for user-defined periods of time, with typically longer trapping times for higher resolution applications. It has previously been suggested that the extended trapping times and applied electric fields may increase the internal energy of ions, resulting in restructuring or even fragmentation of smaller ions.[48] This raises concern when performing nMS experiments, in which maintaining the native-like structure and avoiding unintentional activation are of critical importance.[29,50,51] It has since been clarified that ion

https://doi.org/10.1021/acs.analchem.0c05373
Anal. Chem. 2021, 93, 5513−5520

heating likely occurs due to non-intrinsic properties of TIMS (space charge effects and RF power absorption) and that careful tuning prevents structural rearrangement, therefore making TIMS a suitable technology for nMS.[51] For the experiments performed in this manuscript, the amplitude of the RF-confining voltage in the TIMS funnel was set as low as possible, while still trapping a sufficient amount of ions, and trapping times in the TIMS analyzer were kept low to limit structural perturbation.[29] To confirm the results from Bleiholder and co-workers, TIMS−SID was performed using CTB, a 58 kDa pentamer, with bound GM1s ligands and compared to TIMS−CID of the same complex (TIMS parameters were identical for both TIMS−SID and TIMS−CID experiments). The CTB complex binds five GM1s molecules, each located between two neighboring subunits. The results for CTB with GM1s are shown in Figure 4, and the results agree well with those obtained previously on an Orbitrap with SID installed (monomers retain 0, 1, and 2 ligands and dimers retain 1, 2, and 3 ligands, and so forth, consistent with the fact that the ligands bind at the interface of two protein monomers). Deconvolution of the CTB + GM1s mass spectra was performed by integrating the area under each peak and normalizing against total intensity in OriginPro 9.[52] The full mass spectrum for charge-reduced CTB with GM1s is shown in Figure S8.

Pre-activation of a protein complex can often be probed by SID. Loss of the native-like structure by pre-activation (unintential CID) typically results in an SID spectrum that is more consistent with CID products, that is, disproportionately high-charged monomer and the corresponding $(n - 1)$mer because the complex has been restructured prior to SID. Additionally, pre-activation can lead to ligand loss from the complex. TIMS−CID of the 14+ CTB with the GM1s complex yields the expected highly charged monomer and corresponding tetramer, which further undergo ligand loss (Figure 4B,B2,D). Conversely, TIMS−SID of CTB with GM1s yields a monomer, dimer, trimer, and tetramer, indicative of the equal interfaces between each subunit.[43] For CTB with GM1s, the GM1s ligand binds between individual subunits; therefore, SID results in a monomer with 0, 1, or 2 GM1s bound, dimer with 1, 2, or 3 GM1s bound, and so forth (Figure 4C,C2,E).[53] The observation of charge-symmetric products and retention of the ligand further suggest that carefully tuned TIMS parameters do not result in significant, measurable restructuring of protein complexes. Additionally, ICR instrument parameters downstream from the TIMS funnel were all tuned using low voltages to prevent any inadvertent activation. We likely see less-measurable rearrangement for protein complexes due to their higher barrier for intracomplex rearrangement to occur compared to thermometer ions or monomeric proteins, at least within a 15−34 ms time scale.[54]

It is important to note that a current limitation of this technology is performing IMS directly after ionization without the capabilities of performing an in-source activation step to "clean up" biological samples that contain several non-specific adducts. Heavily adducted samples result in a broad mobility distribution with lower total ion intensity spread across that distribution, making mobility parking on a specific point to couple with SID difficult due to low initial signal intensity. Solution-phase clean up (size exclusion buffer exchange columns), and smaller diameter openings of nanoelectrospray capillaries were used to limit sample contamination in the work presented above. In the future, this technology will be most beneficial when investigating dynamic protein complexes, such as those that exhibit different conformations upon ligand binding or post-translational modifications and that require ultrahigh mass resolution to decipher such small mass differences between those systems.

TIMS−SID of desArg1 and desArg9 Bradykinin. Bradykinin is a peptide composed of nine amino acids (RPPGFSPFR). Removal of the C-terminal arginine (desArg9 or desR9) or the N-terminal arginine (desArg1 or desR1) results in two distinct peptides with the same exact mass. As a result, the two peptides cannot be separated using an analytical quadrupole. TIMS was performed on a 1:1 mixture of desArg1 and desArg9 bradykinin (Figure 5A), and two distinct distributions were observed for the doubly charged peptides. Each distribution was mobility-selected, and SID was performed (Figure 5B,C).

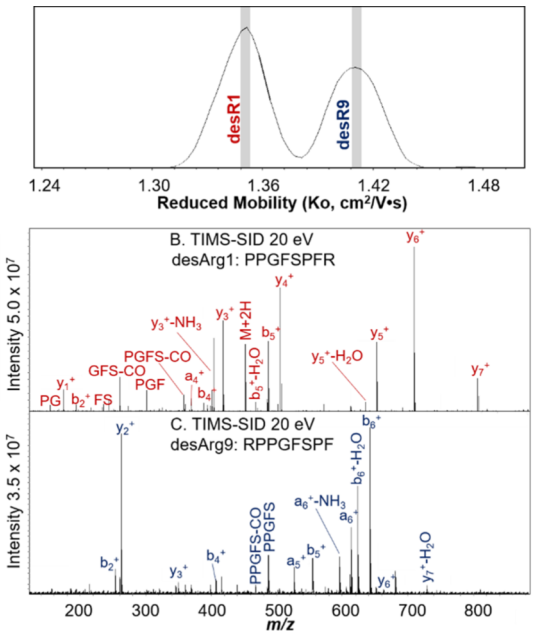

Figure 5. TIMS of a 1:1 mixture of desArg1 and desArg9 bradykinin yielded baseline-resolved distributions of the isobaric peptides (A). Reduced mobilities were calculated using Tune Mix as a calibrant. Each distribution was selected (as indicated by gray slices), and the corresponding peptide was assigned based on the SID fragmentation spectra (B,C).

Using TIMS, we observed baseline IMS resolution for desArg1 and desArg9 bradykinin, previously unachieved on a TWIMS platform.[55] Despite having the same nominal mass, desArg1 and desArg9 bradykinin yield significantly different SID spectra, as we have previously noted. CID and SID spectra of each of these small peptides are similar (desArg1 CID similar to desArg1 SID) with either type of spectra differing for the two isomers. Most notable is the preferential formation of y-type ions from desArg1 because the charge is sequestered on the C-terminal arginine. Comparatively, desArg9 preferentially forms more b-type fragment ions due to charge retention on the N-terminal arginine. Here, TIMS−SID is used for both the separation and identification of isobaric mixtures. The identification of the peptides was also confirmed by performing TIMS on the individual species (Figure S9). It was observed that the peptides, with masses lower than those of the protein complexes, were more sensitive to RF confining amplitude, as evidenced by intact peptide dissociating in the TIMS funnel at

https://doi.org/10.1021/acs.analchem.0c05373
Anal. Chem. 2021, 93, 5513−5520

very high amplitudes. Low RF amplitude (70 V_{pp} for bradykinin compared to 250 V_{pp} for protein complexes) that did not yield any unintentional fragmentation was used for the results presented here. TIMS–SID shows promising potential application in the analysis of complex mixtures that consist of isobaric species that can be identified based on their fragmentation patterns, not just for nMS applications. TIMS also offers the advantages of being a rapid separation technique that does not require excessive amounts of the sample or solvent, compared to traditional liquid chromatography methods used for mixture analysis.

CONCLUSIONS

Various protein complexes and a peptide mixture were successfully trapped and mobility-selected using TIMS on an ultrahigh-resolution 15 T FT-ICR MS platform, further equipped with SID capabilities. The combination of TIMS and SID provided complementary structural information regarding the topology and conformation (relative drift times) of the protein complexes studied. Additionally, TIMS–SID allowed for the separation, fragmentation, and identification of peptide structural isomers present in a mixture. The SID spectra of apo streptavidin and CTB with the GM1s ligand following IM parking were nearly identical to those from quadrupole isolation without any TIMS analysis, suggesting that little to no measurable restructuring or unfolding of protein complexes was observed during the TIMS analysis, supporting the conclusion that TIMS is applicable to nMS experiments in agreement with Bleiholder and co-workers.[51,56] When analyzing peptides, however, RF V_{pp} must be optimized to avoid unintentional ion activation (and possibly fragmentation) due to RF heating. Additionally, the implementation of TIMS–SID on an ultrahigh-resolution platform allows for identification and relative quantification of overlapping oligomeric SID products that would otherwise require a second stage of ion mobility for deconvolution.

ASSOCIATED CONTENT

Supporting Information

The Supporting Information is available free of charge at https://pubs.acs.org/doi/10.1021/acs.analchem.0c05373.

SID device tune settings, TIMS voltage settings, TIMS ramp voltage profile, comparison of mobility calibration curves, CCS determination, CCS values of streptavidin and CTB, FT-ICR tune settings, streptavidin full mass spectrum, streptavidin TIMS–SID and TIMS–CID comparison, CTB with GM1 full mass spectrum, and desArg bradykinin individual mobility distributions (PDF)

AUTHOR INFORMATION

Corresponding Author

Vicki H. Wysocki − *Department of Chemistry and Biochemistry, Resource for Native MS Guided Structural Biology, and Campus Chemical Instrument Center, Mass Spectrometry and Proteomics, The Ohio State University, Columbus, Ohio 43210, United States;* orcid.org/0000-0003-0495-2538; Phone: 614-292-8687; Email: wysocki.11@osu.edu

Authors

Erin M. Panczyk − *Department of Chemistry and Biochemistry and Resource for Native MS Guided Structural Biology, The Ohio State University, Columbus, Ohio 43210, United States;* orcid.org/0000-0003-3779-6738

Dalton T. Snyder − *Resource for Native MS Guided Structural Biology, The Ohio State University, Columbus, Ohio 43210, United States*

Mark E. Ridgeway − *Bruker Daltonics Inc., Billerica, Massachusetts 01821, United States*

Árpád Somogyi − *Campus Chemical Instrument Center, Mass Spectrometry and Proteomics and Resource for Native MS Guided Structural Biology, The Ohio State University, Columbus, Ohio 43210, United States*

Melvin A. Park − *Bruker Daltonics Inc., Billerica, Massachusetts 01821, United States*

Complete contact information is available at: https://pubs.acs.org/10.1021/acs.analchem.0c05373

Notes

The authors declare the following competing financial interest(s): Authors Melvin A. Park and Mark E. Ridgeway work for Bruker Daltonics, the manufacturer of the SolariX 15 T FT-ICR and TIMS analyzer.

ACKNOWLEDGMENTS

The authors would like to thank Jacob Meier (Bruker Daltonics) for help in installing the TIMS device and Desmond Kaplan (KapScience) for thoughtful discussion and advice when coupling TIMS with SID. The FT-ICR was purchased using funds from NIH award S10 OD018507. This work was supported by the NIH Resource for nMS Guided Structural Biology, P41GM128577 (V.H.W.).

REFERENCES

(1) Liko, I.; Allison, T. M.; Hopper, J. T. S.; Robinson, C. V. *Curr. Opin. Struct. Biol.* **2016**, *40*, 136–144.
(2) Lössl, P.; Waterbeemd, M.; Heck, A. J. *EMBO J.* **2016**, *35*, 2634–2657.
(3) Rostom, A. A.; Robinson, C. V. *J. Am. Chem. Soc.* **1999**, *121*, 4718–4719.
(4) Shoemaker, S. C.; Ando, N. *Biochemistry* **2018**, *57*, 277–285.
(5) Ilag, L. L.; Videler, H.; McKay, A. R.; Sobott, F.; Fucini, P.; Nierhaus, K. H.; Robinson, C. V. *Proc. Natl. Acad. Sci. U.S.A.* **2005**, *102*, 8192–8197.
(6) Hernández, H.; Makarova, O. V.; Makarov, E. M.; Morgner, N.; Muto, Y.; Krummel, D. P.; Robinson, C. V. *PLoS One* **2009**, *4*, No. e7202.
(7) Jiang, J.; Chan, H.; Cash, D. D.; Miracco, E. J.; Ogorzalek Loo, R. R.; Upton, H. E.; Casicio, D.; Johnson, R. O.; Collins, K.; Loo, J. A.; Zhou, H.; Feigon, J. *Science* **2015**, *350*, aab4070.
(8) Lorenzen, K.; Olia, A. S.; Uetrecht, C.; Cingolani, G.; Heck, A. J. R. *J. Mol. Biol.* **2008**, *379*, 385–396.
(9) Lanucara, F.; Holman, S. W.; Gray, C. J.; Eyers, C. E. *Nat. Chem.* **2014**, *6*, 281–294.
(10) Song, Y.; Nelp, M. T.; Bandarian, V.; Wysocki, V. H. *ACS Cent. Sci.* **2015**, *1*, 477–487.
(11) Jurneczko, E.; Barran, P. E. *Analyst* **2011**, *136*, 20–28.
(12) Revercomb, H. E.; Mason, E. A. *Anal. Chem.* **1975**, *47*, 970–983.
(13) Mason, E. A.; McDaniel, E. W. *Transport Properties of Ions in Gases*; Wiley: New York, 1988.
(14) Viehland, L. A.; Mason, E. A. *At. Data Nucl. Data Tables* **1995**, *60*, 37–95.

(15) McDaniel, E. W.; Martin, D. W.; Barnes, W. S. *Rev. Sci. Instrum.* **1962**, *33*, 2.
(16) Mesleh, M. F.; Hunter, J. M.; Shvartsburg, A. A.; Schatz, G. C.; Jarrold, M. F. *Anal. Chem.* **1996**, *100*, 16082−16086.
(17) Wyttenbach, T.; Bleiholder, C.; Bowers, M. T. *Anal. Chem.* **2013**, *85*, 2191−2199.
(18) Bleiholder, C.; Johnson, N. R.; Contreras, S.; Wyttenbach, T.; Bowers, M. T. *Anal. Chem.* **2015**, *87*, 7196−7203.
(19) Clemmer, D. E.; Jarrold, M. F. *J. Mass Spectrom.* **1997**, *32*, 577−592.
(20) Gabelica, V.; Marklund, E. *Curr. Opin. Chem. Biol.* **2018**, *42*, 51−59.
(21) Stiving, A. Q.; Jones, B. J.; Ujma, J.; Giles, K.; Wysocki, V. H. *Anal. Chem.* **2020**, *92*, 4475−4483.
(22) Campuzano, I. D. G.; Giles, K. *TrAC, Trends Anal. Chem.* **2019**, *120*, 115620.
(23) Allen, S. J.; Giles, K.; Gilbert, T.; Bush, M. F. *Analyst* **2016**, *141*, 884−891.
(24) Benigni, P.; Marin, R.; Molano-Arevalo, J. C.; Garabedian, A.; Wolff, J. J.; Ridgeway, M. E.; Park, M. A.; Fernandez-Lima, F. *Int. J. Ion Mobility Spectrom.* **2016**, *19*, 95−104.
(25) Liu, F. C.; Cropley, T. C.; Ridgeway, M. E.; Park, M. A.; Bleiholder, C. *Anal. Chem.* **2020**, *92*, 4459−4467.
(26) Michelmann, K.; Silveira, J. A.; Ridgeway, M. E.; Park, M. A. *J. Am. Soc. Mass Spectrom.* **2014**, *26*, 14−24.
(27) Fernandez-Lima, F.; Kaplan, D. A.; Suetering, J.; Park, M. A. *Int. J. Ion Mobility Spectrom.* **2011**, *14*, 93−98.
(28) Ridgeway, M. E.; Lubeck, M.; Jordens, J.; Mann, M.; Park, M. A. *Int. J. Mass Spectrom.* **2018**, *425*, 22−35.
(29) Ridgeway, M. E.; Wolff, J. J.; Silveira, J. A.; Lin, C.; Costello, C. E.; Park, M. A. *Int. J. Ion Mobility Spectrom.* **2016**, *19*, 77−85.
(30) Ridgeway, M. E.; Silveira, J. A.; Meier, J. E.; Park, M. A. *Analyst* **2015**, *140*, 6964.
(31) Ujma, J.; Giles, K.; Morris, M.; Barran, P. E. *Anal. Chem.* **2016**, *88*, 9469−9478.
(32) Koeniger, S. L.; Merenbloom, S. I.; Clemmer, D. E. *J. Phys. Chem. B* **2006**, *110*, 7017−7021.
(33) Koeniger, S. L.; Clemmer, D. E. *J. Am. Soc. Mass Spectrom.* **2007**, *18*, 322−331.
(34) Hernandez, D. R.; DeBord, J. D.; Ridgeway, M. E.; Kaplan, D. A.; Park, M. A.; Fernandez-Lima, F. *Analyst* **2014**, *139*, 1913−1921.
(35) Stiving, A. Q.; VanAernum, Z. L.; Busch, F.; Harvey, S. R.; Sarni, S. H.; Wysocki, V. H. *Anal. Chem.* **2019**, *91*, 190−209.
(36) Zhou, M.; Yan, J.; Romano, C. A.; Tebo, B. M.; Wysocki, V. H.; Paša-Tolić, L. *J. Am. Soc. Mass Spectrom.* **2018**, *29*, 723−733.
(37) Harvey, S. R.; Liu, Y.; Liu, W.; Wysocki, V. H.; Laganowsky, A. *Chem. Commun.* **2017**, *53*, 3106−3109.
(38) Ma, X.; Loo, J. A.; Wysocki, V. H. *Int. J. Mass Spectrom.* **2015**, *377*, 201−204.
(39) Ma, X.; Zhou, M.; Wysocki, V. H. *J. Am. Soc. Mass Spectrom.* **2014**, *25*, 368−379.
(40) Zhou, M.; Wysocki, V. H. *Acc. Chem. Res.* **2014**, *47*, 1010−1018.
(41) Quintyn, R. S.; Zhou, M.; Yan, J.; Wysocki, V. H. *Anal. Chem.* **2015**, *87*, 11879−11886.
(42) Snyder, D. T.; Panczyk, E. M.; Somogyi, A.; Kaplan, D. A.; Wysocki, V. *Anal. Chem.* **2020**, *92*, 11195−11203.
(43) Yan, J.; Zhou, M.; Gilbert, J. D.; Wolff, J. J.; Somogyi, Á.; Pedder, R. E.; Quintyn, R. S.; Morrison, L. J.; Easterling, M. L.; Paša-Tolić, L.; Wysocki, V. H. *Anal. Chem.* **2017**, *89*, 895−901.
(44) Snyder, D. T.; Panczyk, E.; Stiving, A. Q.; Gilbert, J. D.; Somogyi, A.; Kaplan, D.; Wysocki, V. *Anal. Chem.* **2019**, *91*, 14049−14057.
(45) Zhou, M.; Huang, C.; Wysocki, V. H. *Anal. Chem.* **2012**, *84*, 6016−6023.
(46) Hall, Z.; Robinson, C. V. *J. Am. Soc. Mass Spectrom.* **2012**, *23*, 1161−1168.
(47) Stiving, A. Q.; Gilbert, J. D.; Jones, B. J.; Wysocki, V. H. *J. Am. Soc. Mass Spectrom.* **2020**, *31*, 458−462.
(48) Kelly, R. T.; Tolmachev, A. V.; Page, J. S.; Tang, K.; Smith, R. D. *Mass Spectrom. Rev.* **2010**, *29*, 294−312.
(49) Quintyn, R. S.; Yan, J.; Wysocki, V. H. *Chem. Biol.* **2015**, *22*, 583−592.
(50) Morsa, D.; Hanozin, E.; Eppe, G.; Quinton, L.; Gabelica, V.; Pauw, E. D. *Anal. Chem.* **2020**, *92*, 4573−4582.
(51) Bleiholder, C.; Liu, F. C.; Chai, M. *Anal. Chem.* **2020**, *92*, 16329−16333.
(52) *Origin (Pro)*, version 9.0; OriginLab Corporation: Northampton, MA, USA; 2012.
(53) Busch, F.; VanAernum, Z. L.; Ju, Y.; Yan, J.; Gilbert, J. D.; Quintyn, R. S.; Bern, M.; Wysocki, V. H. *Anal. Chem.* **2018**, *90*, 12796−12801.
(54) Harvey, S. R.; Yan, J.; Brown, J. M.; Hoyes, E.; Wysocki, V. H. *Anal. Chem.* **2016**, *88*, 1218−1221.
(55) Stiving, A. Q.; Harvey, S. R.; Jones, B. J.; Bellina, B.; Brown, J. M.; Barran, P. E.; Wysocki, V. H. *J. Am. Soc. Mass Spectrom.* **2020**, *31*, 2313−2320.
(56) Jeanne Dit Fouque, K.; Garabedian, A.; Leng, F.; Tse-Dinh, Y.-C.; Ridgeway, M. E.; Park, M. A.; Fernandez-Lima, F. *Anal. Chem.* **2021**, *93* (5), 2933−2941.

https://doi.org/10.1021/acs.analchem.0c05373
Anal. Chem. 2021, 93, 5513−5520